Int J Clin Exp Med 2016;9(7):13584-13594
www.ijcem.com /ISSN:1940-5901/IJCEM0025615

Original Article

Dual-intelligent functionalized silica nanoparticles for liver cancer imaging and therapy

Xuya Zhao, Shi Zhou, Dazhi Wang, Wei He, Junxiang Li, Shuai Zhang

Department of Interventional Radiology, Guizhou Cancer Hospital, Cancer Hospital of Guizhou Medical University, Guiyang 550003, China

Received February 4, 2016; Accepted June 8, 2016; Epub July 15, 2016; Published July 30, 2016

Abstract: A novel strategy to construct a therapeutic system based on functionalized SLNs which can specifically respond to tumor microenvironment was reported. In the therapeutic system, doxorubicin was conjugated to SLNs via disulfide bond by using a peptide substrate, CPLGLAGG, which can be specifically cleaved by the MMP-2 protease. *In vitro* and *in vivo* study in HepG2 cells and HepG2 tumor-bearing mice show that over-expressed protease of MMP-2 in tumor tissue and intracellular GSH can lead to the rapid release of the anti-tumor drug (doxorubicin) from the functionalized SLNs, simultaneously realizing inhibition of tumor growth and fluorescently imaging, which in turn, can further improve the anti-tumor efficacy and reduce side effects significantly.

Keywords: Liver cancer, silica nanoparticles, imaging, doxorubicin, peptide substrate

Introduction

Liver cancer is one of most deadly cancers worldwide, which responsible to more than 732000 deaths across the world in 2013 alone [1]. Although chemotherapy is considered as one of the most commonly applied approach to treat cancer, the inefficient and unspecific delivery of chemotherapeutic drugs usually limits its therapeutic efficacy and leads to unwanted side effects [2]. To overcome these limitations, many efforts have been recently devoted to seek multifunctional devices for versatile cancer therapy [3, 4]. In particular, functionalized silica nanoparticles (SLNs) have attracted great interest in research due to their well biocompatibility, great optical properties and excellent potential in biomedical applications, especially cancer therapy, as diagnostic agents and drug carriers [5, 6]. Furthermore, the functionalized SLNs with reasonable modification can intelligently release the drug in response to external stimuli, including pH, light, and competitive molecules (such as glutathione (GSH)) [7-9]. There has been an increasing research interest to combine cancer treatment and diagnosis within one nanocarrier platform simultaneously, which holds great potential to revolutionize cancer therapy and diagnosis [10, 11].

In this regard, the dual-intelligent SLNs which on one hand response to the microenvironment distinction of tumor sites, and on the other hand realize fluorescent imaging were developed. It has been well established that some enzymes, such as the matrix metalloproteinases (MMPs), are overexpressed in tumor which play critical role in tumor progressing and are crucial to extracellular matrix remodeling [12, 13]. Therefore, the MMP-2 protease sensitive SLNs were designed and prepared. Firstly, a peptide substrate, CPLGLAGG, which can be specifically cleaved by MMP-2 [14], was employed as linker to conjugate anti-cancer drug doxorubicin (Dox) to SLNs via disulfide bond. Owing to self-quenching effect, the fluorescence of Dox can be quenched once Dox is absorbed onto or into the SLNs [15, 16]. After arriving at tumor sites, the overexpressed MMP-2 protease can readily hydrolyze the peptide substrate to trigger the release of Dox, which results in pronounced fluorescence of Dox recovered from quenching state to exciting state. This switchable fluorescence property can be applied for tumor imaging, at the same

time, the released Dox can exert its therapeutic effect to achieve tumor inhibition. Besides, the disulfide bond between the peptide substrate and SLNs, when these SLNs are internalized by tumor cells via endocytosis, can realize accelerated release of Dox to improve the anti-tumor efficiency using the exchange reaction between disulfide bond and the abundant glutathione (GSH) in the cytoplasm. Noted here, an ideal therapeutic system based on SLNs we designed is capable of inducing the accelerated release of Dox from SLNs with switchable fluorescence of Dox from quenching to exciting, which can simultaneously realize *in vivo* cancer imaging and therapy.

Materials and methods

Materials

Triton X-100, tetraethyl orthosilicate (TEOS), (3-mercaptopropyl)-trimethoxysilane (MPTMS) were obtained from Sigma Aldrich (St. Louis, MO, USA). Doxorubicin hydrochloride was purchased from Zhejiang Hisun Pharmaceutical Co. (Taizhou, China), 1,10-phenanthroline monohydrate and tecnazene (TCNB) were purchased from Aladdin Reagent Co. Ltd. (Shanghai, China). Matrix metalloproteinase (MMP-2), glutathione (GSH), TIMP-2, 1,10-phenanthroline monohydrate, 3-[4,5-Dimethylthiazol-2-yl]-2,5-diphenyltetra-zoliumbromide (MTT), DMEM medium, fetal bovine serum (FBS), penicillin streptomycin, trypsin, molecular probe (Hoechst 33258) and Dulbecco's phosphate buffered saline (PBS) were purchased from Invitrogen (California, USA). All other reagents and solvents were of analytical grade and provided by Shanghai Chemical Co. (Shanghai, China).

Synthesis of the peptide Ac-Cys(Trt)-Pro-Leu-Gly-Leu-Ala-Gly-Gly-OH

The peptide Ac-Cys(Trt)-Pro-Leu-Gly-Leu-Ala-Gly-Gly-OH was synthesized manually by standard Fmoc solid phase peptide synthesis according to previous reported method [14].

Synthesis and purification of the protease sensitive peptide substrate Ac-Cys-Pro-Leu-Gly-Leu-Ala-Gly-Gly-Dox

The peptide substrate Ac-Cys-Pro-Leu-Gly-Leu-Ala-Gly-Gly-Dox was prepared by reacting the peptide with doxorubicin hydrochloride in dimethylformamide (DMF) using a standing coupling procedure as reported previously [14].

Preparation of SSLNs

Thiol-terminated silica nanoparticles (SSLNs) were directly synthesized according to previous report with minor modifications [17] by using the synchronous hydrolysis of TEOS and MPTMS in water-in-oil microemulsion. Briefly, a water-in-oil microemulsion was prepared by mixing 1.8 ml Triton X-100, 7.5 ml cyclohexane, 1.6 ml n-hexanol, and 480 μL of water. After stirring for 0.5 h, 180 μL TEOS and 60 μL MPTMS were then added as precursors for silica matrix formation, followed by the addition of 100 μl NH_4OH to initiate the polymerization process. The reaction was allowed to continue for 24 h at room temperature. After that, the SSLNs were precipitated by addition of ethanol and were washed with ethanol and water respectively for several times to remove the surfactant from the particles.

Preparation of Dox-peptide/SSLN

The protease sensitive functionalized silica nanoparticle (Dox-peptide/SSLN) was prepared by using the covalent bonding interactions between the thiol groups of peptides and SLNs. The protease sensitive peptide substrate (Dox-peptide) was dissolved in water at a concentration of 6 μM, then 9 nM of SLNs was added to Dox-peptide solution under stirring for 24 h at room temperature with the protection of nitrogen. After that, the mixture was dialyzed in a dialysis bag (MWCO: 14,000 Da) against DI water (2 L × 3) followed by lyophilization to obtain Dox-peptide/SSLN.

Characterization of SSLNs and Dox-peptide/SSLN

Dynamic light scattering (DLS) techniques with a Zetasizer Nano ZS (Malvern Instruments, UK) was employed to measure the particle size of SSLNs and Dox-peptide/SSLN. The morphologies were further observed by transmission electron microscopy (TEM) under an Electron Microscope (JEM-2100, JEOL, Japan). Thermal gravitational analysis (TGA) was performed with a thermal analyzer (TGS-II, PerkineElmer, USA) to analyze the content of Dox-peptide in Dox-peptide/SSLN and to calculate the Dox loading efficiency.

In vitro release of Dox

The release of Dox under external stimuli of MMP-2 and GSH was performed as reported previously [14]. In brief, 2 ml of Dox-peptide/SSLN solution were suspended in four different media: (a) 2 ml TCNB buffer containing MMP-2 (2 μg/mL, 100 μL); (b) TCNB buffer (2 mL) with 10 mm GSH; (c) TCNB buffer (2 ml) containing MMP-2 (2 μg/mL, 100 μL) and MMP-2 protease inhibitor 1,10-phenanthroline monohydrate (1 mm); (d) TCNB buffer (2 ml), respectively, and transferred into dialysis tubes (MWCO: 14,000 Da). Subsequently, the dialysis tube was immersed in 10 ml of TCNB buffer solution and incubated at 37°C. The incubation medium was analyzed by spectrofluorophotometer (UV2450, Shimadzu, Japan) at λ_{ex} = 470 nm at pre-determined time intervals.

Cell culture

HepG2 cells (Human hepatoma cells) incubated in DMEM supplied with 10% FBS and 1% antibiotics (penicillin-streptomycin, 10,000 U/mL) were placed at 37°C in a humidified atmosphere with 5% CO_2.

In vitro cytotoxicity of Dox-peptide/SSLN

In vitro cytotoxicity was performed with HepG2 cells by standard MTT assay. Briefly, HepG2 cells were seeded at a density of 1×10^3 cells per well in 96-well plates and cultured overnight at 37°C in 200 μL of culture medium. Afterwards, the medium was removed, and the cells were incubated for 48 h in a serum-free medium containing Dox-peptide/SSLN at various concentrations. Then, 20 μL of MTT solution (5 mg/ml) was added to each well, and the cells were further incubated for 4 hours. The supernatant in the wells was discarded, and 150 μl of DMSO was added to dissolve the substrate for 10 minutes. The absorbance in each well was recorded at 570 nm using a microplate reader (Bio-rad 680, Bio-rad, USA) [18].

Cellular uptake of Dox-peptide/SSLN

HepG2 cells were seeded in a glass bottom dish at a density of 1×10^5 cells/well and cultured overnight to give 60%-70% confluence. Thereafter, Dox-peptide/SSLN (containing 1.5 μg/ml of Dox) dispersed in culture medium was added with further incubated at 37°C for another 4 h. After removing the medium and washing with PBS, cells were stained by Hoechst 33258 for 20 min and observed using Confocal Laser Scanning Microscopy (CLSM, Nikon C1-si, BD Laser, USA). To further determine the MMP-2 related internalization of Dox-peptide/SSLN, HepG2 cells were pretreated with MMP-2 protease inhibitor TIMP-2 0.5 h before the addition of Dox-peptide/SSLN.

Flow cytometry analysis

HepG2 cells were seeded in 24-well plates at a density of 5×10^4 cells/well overnight. Then all cells were incubated with Dox-peptide/SSLN (1.5 μg/mL of free Dox) for another 4 h. After that, the medium was discarded and the cells were washed thoroughly with PBS. Then all the cells were suspended by trypsin and collected within centrifuge tubes by centrifugation. The cells were re-suspended and subjected to red fluorescence determination by flow cytometry (TM III, FACSAria, USA).

In vivo optical imaging

BALB/c nude mice (5-weeks old, Shanghai Laboratory Animal Center, Shanghai, China) were used for animal experiments. Subcutaneous tumors were established by injecting HepG2 (1×10^6 cells in 200 μL PBS) into the flank of mice [19]. When tumors reached approximately 100 mm^3 in volume, 100 μl of Dox-peptide/SSLN (Dox dosage: 5 mg/kg) in PBS (pH 7.4) were subcutaneous injected. To confirm that the MMP-2 is related to the restore of fluorescence of Dox, TIMP-2 was intratumorally administered into the HepG2 tumors 0.5 h prior to the injection of Dox-peptide/SSLN. The optical images were obtained with an *in vivo* imaging system (FXPRO, Kodak, USA) using 465-529 nm excitation and 565 nm long-pass emission filters [14].

Therapeutic efficacy of Dox-peptide/SSLN in HepG2 tumor-bearing mice

To further study the therapeutic efficacy of Dox-peptide/SSLN, the tumor-bearing mice model established as mentioned in the above Section was employed when the tumor volume approximately reached 100 mm^3. The mice were randomly divided into four groups, which are phosphate buffered saline (PBS), free Dox and Dox-

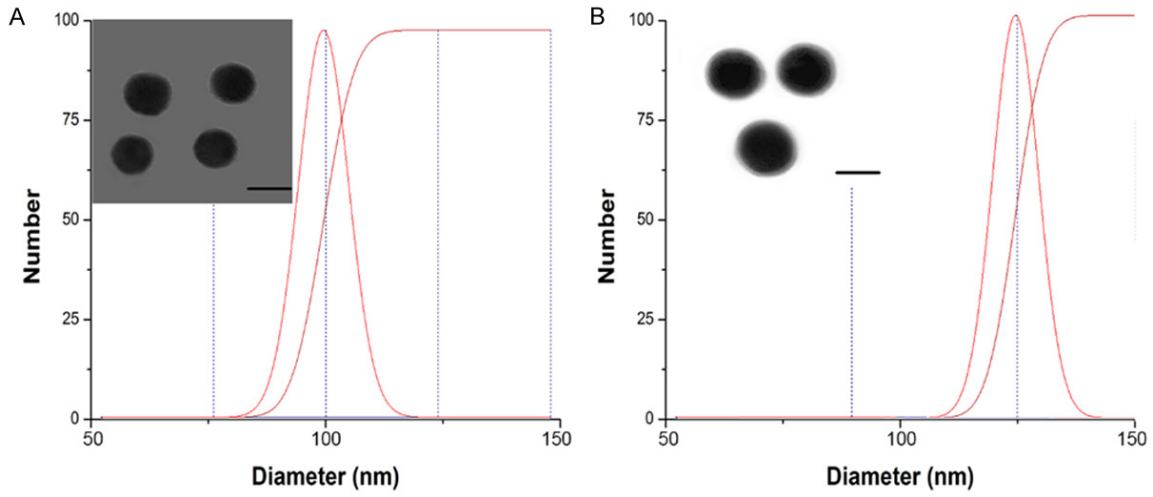

Figure 1. Particle size distribution and morphology of (A) SSLNs and (B) Dox-peptide/SSLN. Scale bar: 100 nm.

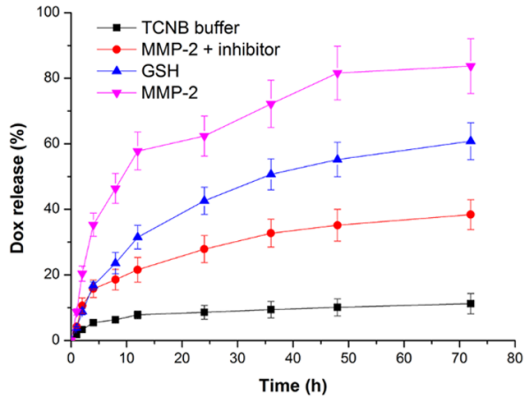

Figure 2. Release profile of Dox from Dox-peptide/SSLN in different media: (1) TCNB buffer. (2) TCNB buffer with MMP-2 (2 mg/ml) and MMP inhibitor (1,10-phenanthroline monohydrate (1 mm). (3) TCNB buffer with 10 mM GSH. (4) TCNB buffer with 100 μl MMP-2 (2 μg/ml). Data were shown as mean ± S.D. (n = 3).

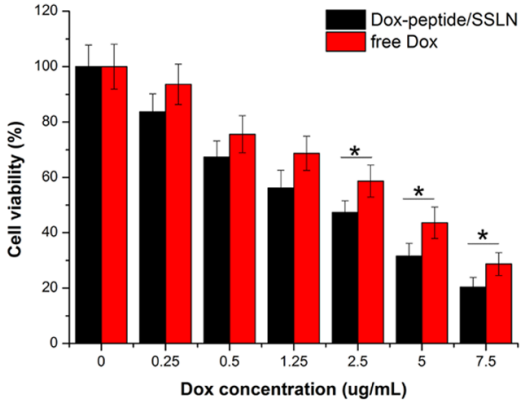

Figure 3. The viability of HepG2 cells incubated with Dox-peptide/SSLN and free Dox for 48 h. Data were shown as mean ± S.D. (n = 3).

peptide/SSLN (Dox dosage: 5.0 mg/kg) with subcutaneous injection. Mice in all groups were injected every 2 days for 14 days. The body weight and tumor growth of every mouse were monitored before the injection. Tumor size was evaluated by measuring perpendicular diameters using a caliper and calculated using the following formula $V = W^2 \times L/2$ (W and L were the shortest and longest diameters, respectively).

Histology analysis

The tumor, heart, liver, spleen, lung and kidney were fixed by 4% formalin and embedded in paraffin and then sectioned. The sections were stained with Hematoxylin/eosin and then pictured by microscopy (Olympus, CX21BIM-SET5, Japan).

Results and discussion

Preparation and characterization of Dox-peptide/SSLN

In this study, mono-dispersed SLNs were fabricated by classical reverse water-in-oil microemulsion method. After conjugation Dox-peptide to the surface of mono-dispersed SSLNs (100 nm), the obtained Dox-peptide/SSLN was characterized by dynamic light scattering (DLS), electronic light scattering (DLS) and transmission electron microscopy (TEM)

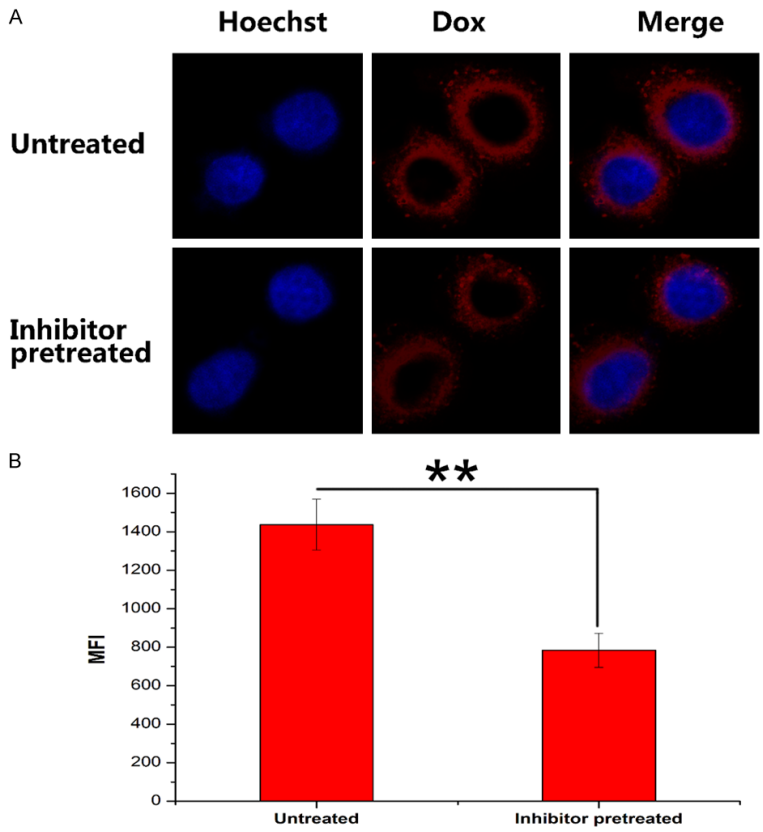

Figure 4. *In vitro* uptake of Dox-peptide/SSLN in HepG2 cells after 4 h of incubation was qualitatively analyzed by (A) CLSM and quantitatively analyzed by (B) flpt cytometry, respectively. Data were shown as mean ± S.D. (n = 3). $P < 0.05$ and $^{**}P < 0.01$.

(**Figure 1**). It was observed that both SSLNs and Dox-peptide/SSLN showed favorable mono-dispersion and stability. It was worth mentioning that compared with SSLNs, the Dox-peptide/SSLN displayed a slightly increase diameter (128 nm) with evident core-shell structure, which indicated that the Dox-peptide was successfully coated to the surface of the SSLNs. On the other hand, thermogravimetric analysis (TGA) indicated that the content of Dox-peptide in Dox-peptide/SSLN was around 6.5 wt% and the amount of Dox loading was 2.8 wt% (data not shown).

In vitro release

CPLGLAGG has been reported to be a preferable linker which can be specifically cleaved by MMP-2 [14]. Since the Dox-peptide substrate was conjugated to SLNs via disulfide bond, when these SLNs are internalized by tumor cells, thiol group exchange behavior between the disulfide bond and the abundant glutathione (GSH) in the cytoplasm is expected to accelerate the Dox release from Dox-peptide/SSLN. It was inferred that when incubating Dox-peptide/SSLN with the protease MMP-2 or the reductive GSH, accelerated Dox release could be observed. As a proof of concept that drug release of Dox-peptide/SSLN is responsive to both protease and reductive, MMP-2 protease and GSH were respectively employed as external stimuli. According to **Figure 2**, it was observe that the Dox released from Dox-peptide/SSLN in the absence of MMP-2 protease and GSH was slow (only 11.2%) within 72 h, revealing that the Dox-peptide/SSLN was highly stable and underwent minimal nonspecific cleavage, which is favorable for its circulation in the blood stream. By contrast, the steady and rapid release of Dox was triggered with the presence of MMP-2 or GSH, and the percentages of accumulated release were approximately 83.7% and 60.8%, respectively, after 72 h. However, when MMP-2 was co-incubated with inhibitor 1, 10-phenanthroline, a MMP-2 inhibitor, the release rate significantly slowed down, which suggested the important role of MMP-2 in the accelerated release of Dox from Dox-peptide/SSLN. It was inferred that Dox-peptide/SSLN was stable in the plasma without releasing the drug after intravenously administered, whereas rapid release of drug could be achieved in tumor cells with the abundant presence MMP-2 and/or GSH, which is favorable in drug delivery.

In vitro anti-tumor effect of Dox-peptide/SSLN

The inhibition ability of Dox-peptide/SSLN to tumor cells was evaluated by MTT assay (**Figure 3**). The results showed that the anti-tumor effect of Dox-peptide/SSLN followed a dose-dependent manner as the viability of HepG2

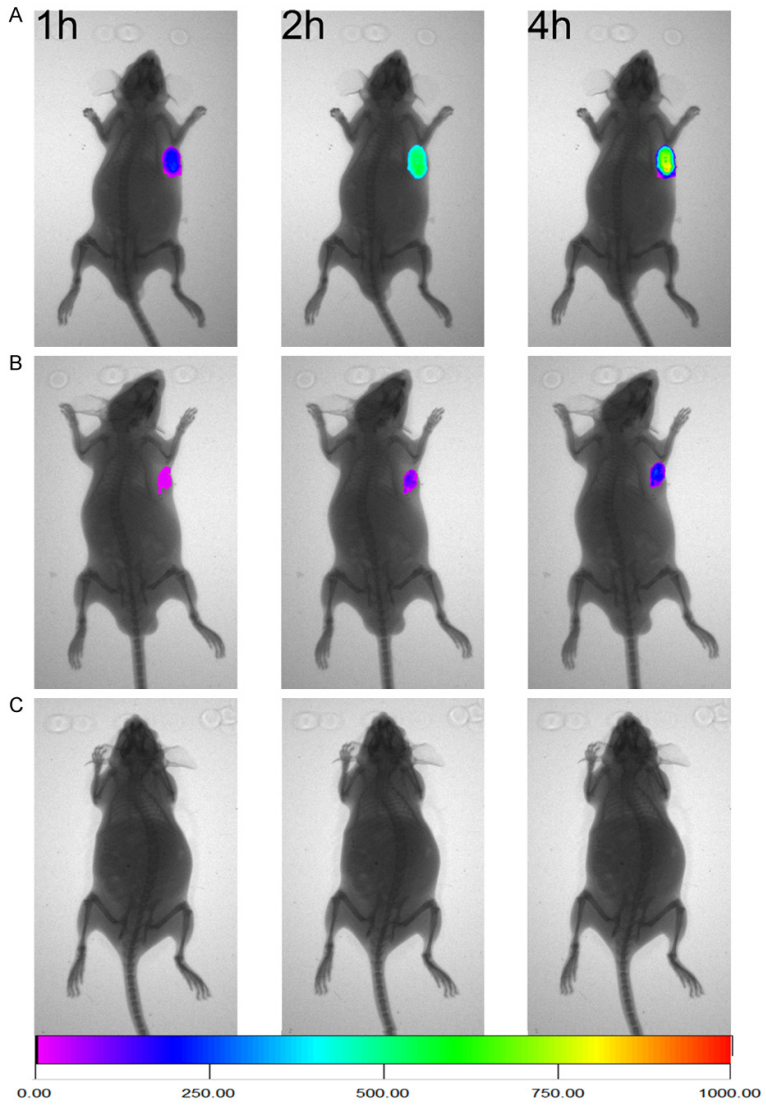

Figure 5. *In vivo* optical images of subcutaneous HepG2 tumor bearing nude mice after injection of Dox-peptide/SSLN without (A) and with (B) inhibitor and the normal mice after injection of the Dox-peptide/SSLN without inhibitor were taken as control (C).

cells decreased with the increase of Dox-peptide/SSLN concentration. The viability of HepG2 cells was around 20.4% after incubation with Dox-peptide/SSLN at a Dox concentration of 7.5 μg/ml for 48 h. It was noted mentioning that compared with free Dox at the same Dox concentration, Dox-peptide/SSLN exerted lower cell viability. This difference in cell viability implied that more Dox in Dox-peptide/SSLN can fully exert its anti-tumor effect than that in free Dox group, inducing more cell apoptosis. This might be attributed to the enhanced uptake of Dox molecule (Dox-peptide/SSLN by-passing the multidrug resistance of HepG2 cells) and the responsive burst-release of Dox from Dox-peptide/SSLN. All these results suggested that Dox-peptide/SSLN have strong capability to enter tumor cells, and at the same time can responsive release Dox, leading to the apoptosis of tumor cells.

In vitro uptake of Dox-peptide/SSLN

The *in vitro* anti-tumor effect of Dox-peptide/SSLN was investigated in HepG2 cells with positive expression of MMP-2 [20]. As displayed in confocal laser scanning microscopy (CLSM) images in **Figure 4**, the red fluorescence of Dox can be observed in both HepG2 cells. To further elucidate the mechanism of internalization, a competitive experiment was performed by treating HepG2 cells with prior to incubation with the nanoparticles. As expected, compared with untreated ones, the cells pretreated with MMP-2 protease inhibitor displayed a significantly drop in fluorescence intensity. The results of flow cytometry quantitative analysis were consistent with CLSM observation. As displayed in **Figure 4B**, the mean fluorescence intensity (MFI) of untreated cells (1437) was higher than that of inhibitor pretreated cells (784). These results indicated that MMP-2 protease is greatly related to the release of Dox from Dox-peptide/SSLN.

In vivo tumor optical imaging of Dox-peptide/SSLN

The *in vivo* tumor imaging of Dox-peptide/SSLN was investigated using HepG2 tumor bearing mice model. To evaluate the *in vivo* imaging possibility, all the mice subcutaneous injected with Dox-peptide/SSLN were subjected to small animal *in vivo* imaging system at predetermined

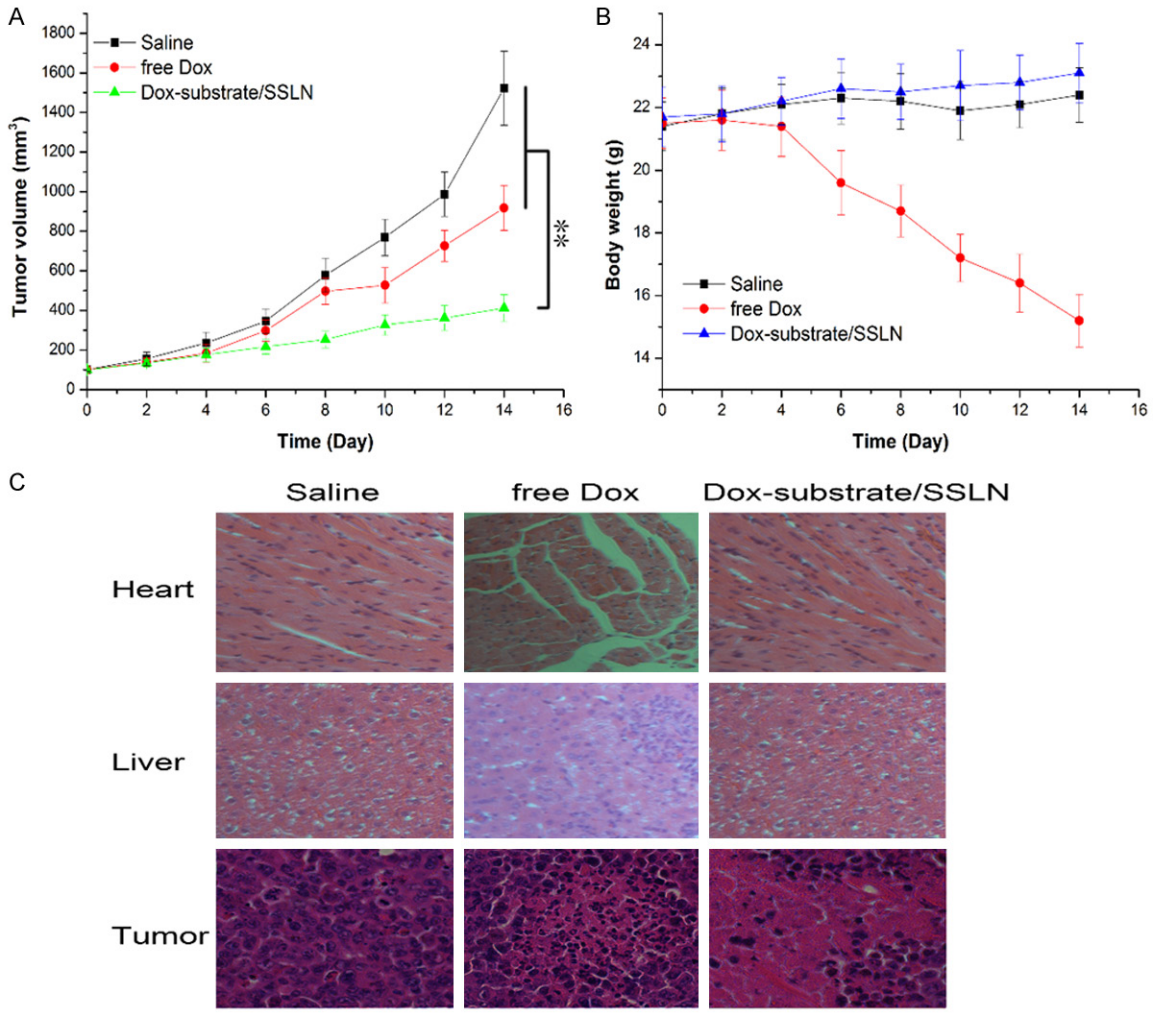

Figure 6. (A) Tumor volume and (B) body weights of HepG2 tumor xenografted nude mice after treatment with Saline, free Dox and Dox-peptide/SSLN (Dox dosage: 5.0 mg/kg), respectively, for a period of 14 days. Data were shown as mean ± S.D. (n = 6). (C) H&E staining images (200×) of the tumor, heart and liver sections of the mice with different treatments. $P < 0.05$ and $^{**}P < 0.01$.

time points. As shown in **Figure 5A**, the fluorescence of Dox could be clear visualized at tumor region after the injection of Dox-peptide/SSLN for 1 h and the fluorescence intensity increased steadily as a function of time. In contrast, for the animal administered with TIMP-2 (the MMP-2 inhibitor) 30 min before the injection of Dox-peptide/SSLN, the fluorescence faded significantly in tumor region (**Figure 5B**). Normal nude mice without tumor model was employed as a control, it was also difficult to observe the flto observe of Dox at the flank upon injection of Dox-peptide/SSLN for 4 h (**Figure 6C**). These results indicated that the Dox is well-preserved within Dox-peptide/SSLN undere normal physiological conditions and released only at the tumor site where over-expressed protease MMP-2 could readily cleave the peptide substrate to recover the fluorescence of Dox. By this way, *in vivo* tumor imaging is realized smartly.

In vivo anti-tumor evaluation of Dox-peptide/SSLN

To evaluate the *in vivo* anti-tumor capability of Dox-peptide/SSLN, subcutaneous tumors were artificially constructed in the flank of BALB/c nude mice by injecting HepG2 cells. Three groups of tumor bearing mice with a single subcutaneous injection (phosphate buffered saline (PBS)), free Dox (5.0 mg/kg) and Dox-peptide/

SSLN were studied. As shown in **Figure 6A**, the relative xenografted tumor volume of Dox-peptide/SSLN group was 412 ± 67 mm^3 after 14-day the treatment, which was rather less than that of the PBS group (1523 ± 187 mm^3). As a control, the tumor volume of the free Dox (5.0 mg/kg) group was 918 ± 114 mm^3. The therapeutic efficacy was further studied by histological examination. Hematoxylin/eosin (H&E) staining (**Figure 6C**) showed that the tumors treated with PBS were composed of abundant acidophilous cells with no obvious damage, which is typically for tumor cells. However, the apoptotic cells and areas of dead cells without nuclei were observed in the tumors treated with free Dox. Moreover, Dox-peptide/SSLN group showed most satisfied results with extensive apoptotic cells and large area of dead cells being obtained. In addition, the body weight of mice in the free Dox group reduced sharply, while the mice in other groups showed no apparent weight changes (**Figure 6B**). This observation implied that Dox-peptide/SSLN did not cause apparent toxicity, whereas the free Dox group showed severe toxicity which comprise the living quality of the mice. It has been widely recognized that the subacute toxicity (such as cardiotoxicity, hepatotoxicity and other toxicities) of free Dox is inevitable in normal chemotherapy [21]. This was also confirmed by H&E staining of heart and liver tissue of the treated animals. It was observed that free Dox exhibited severe myocardial damage and hepatotoxicity characterized as indicated by nuclear shrinkage, cell necrosis and inflammatory cell infiltration. However, the tumor-responsive drug release systems, Dox-peptide/SSLN, can relief this dilemma by ensuring the anti-cancer drug only be released in the tumor region, which can in turn, improve the treatment effect.

Conclusion

In summary, we have designed and prepared a therapeutic system based on functionalized SLNs (Dox-peptide/SSLN) which can response to the microenvironment distinction of tumor sites. The overexpression MMP-2 protease in tumor tissue can hydrolyze nanoparticles, leading to the recovery of the fluorescence of Dox and rapidly release of Dox to realize tumor imaging and therapy. In addition, the thiol exchanging reaction between disulfide bond and intracellular GSH led to accelerated intracellular release of Dox from Dox-peptide/SSLN and enhanced efficacy of *in vivo* tumor imaging and tumor growth inhibition. The Dox-peptide/SSLN with tumor triggered drug release stealth behavior show a great potential in application for cancer therapy and diagnosis.

Disclosure of conflict of interest

None.

Address correspondence to: Shi Zhou, Department of Interventional Radiology, Guizhou Cancer Hospital, Cancer Hospital of Guizhou Medical University, Guiyang 550003, China. E-mail: shizhou1972@sina.com

References

[1] Naghavi M, Wang H, Lozano R, Davis A, Liang X, Zhou M, Vollset SE, Ozgoren AA, Abdalla S, Abd-Allah F, Abdel Aziz MI, Abera SF, Aboyans V, Abraham B, Abraham JP, Abuabara KE, Abubakar I, Abu-Raddad LJ, Abu-Rmeileh NM, Achoki T, Adelekan A, Ademi Z, Adofo K, Adou AK, Adsuar JC, Ärnlov J, Agardh EE, Akena D, Al Khabouri MJ, Alasfoor D, Albittar M, Alegretti MA, Aleman AV, Alemu ZA, Alfonso-Cristancho R, Alhabib S, Ali MK, Ali R, Alla F, Al Lami F, Allebeck P, AlMazroa MA, Al-Shahi Salman R, Alsharif U, Alvarez E, Alviz-Guzman N, Amankwaa AA, Amare AT, Ameli O, Amini H, Ammar W, Anderson HR, Anderson BO, Antonio CA, Anwari P, Apfel H, Argeseanu Cunningham S, Arsic Arsenijevic VS, Artaman A, Asad MM, Asghar RJ, Assadi R, Atkins LS, Atkinson C, Badawi A, Bahit MC, Bakfalouni T, Balakrishnan K, Balalla S, Banerjee A, Barber RM, Barker-Collo SL, Barquera S, Barregard L, Barrero LH, Barrientos-Gutierrez T, Basu A, Basu S, Basulaiman MO, Beardsley J, Bedi N, Beghi E, Bekele T, Bell ML, Benjet C, Bennett DA, Bensenor IM, Benzian H, Bertozzi-Villa A, Beyene TJ, Bhala N, Bhalla A, Bhutta ZA, Bikbov B, Bin Abdulhak A, Biryukov S, Blore JD, Blyth FM, Bohensky MA, Borges G, Bose D, Boufous S, Bourne RR, Boyers LN, Brainin M, Brauer M, Brayne CE, Brazinova A, Breitborde N, Brenner H, Briggs AD, Brown JC, Brugha TS, Buckle GC, Bui LN, Bukhman G, Burch M, Campos Nonato IR, Carabin H, Cárdenas R, Carapetis J, Carpenter DO, Caso V, Castañeda-Orjuela CA, Castro RE, Catalá-López F, Cavalleri F, Chang JC, Charlson FC, Che X, Chen H, Chen Y, Chen JS, Chen Z, Chiang PP, Chimed-Ochir O, Chowdhury R, Christensen H, Christophi CA, Chuang TW, Chugh SS, Cirillo M, Coates MM, Coffeng LE, Coggeshall MS, Cohen A, Colistro

V, Colquhoun SM, Colomar M, Cooper LT, Cooper C, Coppola LM, Cortinovis M, Courville K, Cowie BC, Criqui MH, Crump JA, Cuevas-Nasu L, da Costa Leite I, Dabhadkar KC, Dandona L, Dandona R, Dansereau E, Dargan PI, Dayama A, De la Cruz-Góngora V, de la Vega SF, De Leo D, Degenhardt L, del Pozo-Cruz B, Dellavalle RP, Deribe K, Des Jarlais DC, Dessalegn M, deVeber GA, Dharmaratne SD, Dherani M, Diaz-Ortega JL, Diaz-Torne C, Dicker D, Ding EL, Dokova K, Dorsey ER, Driscoll TR, Duan L, Duber HC, Durrani AM, Ebel BE, Edmond KM, Ellenbogen RG, Elshrek Y, Ermakov SP, Erskine HE, Eshrati B, Esteghamati A, Estep K, Fürst T, Fahimi S, Fahrion AS, Faraon EJ, Farzadfar F, Fay DF, Feigl AB, Feigin VL, Felicio MM, Fereshtehnejad SM, Fernandes JG, Ferrari AJ, Fleming TD, Foigt N, Foreman K, Forouzanfar MH, Fowkes FG, Paleo UF, Franklin RC, Futran ND, Gaffikin L, Gambashidze K, Gankpé FG, García-Guerra FA, Garcia AC, Geleijnse JM, Gessner BD, Gibney KB, Gillum RF, Gilmour S, Ginawi IA, Giroud M, Glaser EL, Goenka S, Gomez Dantes H, Gona P, Gonzalez-Medina D, Guinovart C, Gupta R, Gupta R, Gosselin RA, Gotay CC, Goto A, Gouda HN, Graetz N, Greenwell KF, Gugnani HC, Gunnell D, Gutiérrez RA, Haagsma J, Hafezi-Nejad N, Hagan H, Hagstromer M, Halasa YA, Hamadeh RR, Hamavid H, Hammami M, Hancock J, Hankey GJ, Hansen GM, Harb HL, Harewood H, Haro JM, Havmoeller R, Hay RJ, Hay SI, Hedayati MT, Heredia Pi IB, Heuton KR, Heydarpour P, Higashi H, Hijar M, Hoek HW, Hoffman HJ, Hornberger JC, Hosgood HD, Hossain M, Hotez PJ, Hoy DG, Hsairi M, Hu G, Huang JJ, Huffman MD, Hughes AJ, Husseini A, Huynh C, Iannarone M, Iburg KM, Idrisov BT, Ikeda N, Innos K, Inoue M, Islami F, Ismayilova S, Jacobsen KH, Jassal S, Jayaraman SP, Jensen PN, Jha V, Jiang G, Jiang Y, Jonas JB, Joseph J, Juel K, Kabagambe EK, Kan H, Karch A, Karimkhani C, Karthikeyan G, Kassebaum N, Kaul A, Kawakami N, Kazanjan K, Kazi DS, Kemp AH, Kengne AP, Keren A, Kereselidze M, Khader YS, Khalifa SE, Khan EA, Khan G, Khang YH, Kieling C, Kinfu Y, Kinge JM, Kim D, Kim S, Kivipelto M, Knibbs L, Knudsen AK, Kokubo Y, Kosen S, Kotagal M, Kravchenko MA, Krishnaswami S, Krueger H, Kuate Defo B, Kuipers EJ, Kucuk Bicer B, Kulkarni C, Kulkarni VS, Kumar K, Kumar RB, Kwan GF, Kyu H, Lai T, Lakshmana Balaji A, Lalloo R, Lallukka T, Lam H, Lan Q, Lansingh VC, Larson HJ, Larsson A, Lavados PM, Lawrynowicz AE, Leasher JL, Lee JT, Leigh J, Leinsalu M, Leung R, Levitz C, Li B, Li Y, Li Y, Liddell C, Lim SS, de Lima GM, Lind ML, Lipshultz SE, Liu S, Liu Y, Lloyd BK, Lofgren KT, Logroscino G, London SJ, Lortet-Tieulent J, Lotufo PA, Lucas RM, Lunevicius R, Lyons RA, Ma S, Machado VM, MacIntyre MF, Mackay MT, MacLachlan JH, Magis-Rodriguez C, Mahdi AA, Majdan M, Malekzadeh R, Mangalam S, Mapoma CC, Marape M, Marcenes W, Margono C, Marks GB, Marzan MB, Masci JR, Mashal MT, Masiye F, Mason-Jones AJ, Matzopolous R, Mayosi BM, Mazorodze TT, McGrath JJ, McKay AC, McKee M, McLain A, Meaney PA, Mehndiratta MM, Mejia-Rodriguez F, Melaku YA, Meltzer M, Memish ZA, Mendoza W, Mensah GA, Meretoja A, Mhimbira FA, Miller TR, Mills EJ, Misganaw A, Mishra SK, Mock CN, Moffitt TE, Mohamed Ibrahim N, Mohammad KA, Mokdad AH, Mola GL, Monasta L, Monis Jde L, Montañez Hernandez JC, Montico M, Montine TJ, Mooney MD, Moore AR, Moradi-Lakeh M, Moran AE, Mori R, Moschandreas J, Moturi WN, Moyer ML, Mozaffarian D, Mueller UO, Mukaigawara M, Mullany EC, Murray J, Mustapha A, Naghavi P, Naheed A, Naidoo KS, Naldi L, Nand D, Nangia V, Narayan KM, Nash D, Nasher J, Nejjari C, Nelson RG, Neuhouser M, Neupane SP, Newcomb PA, Newman L, Newton CR, Ng M, Ngalesoni FN, Nguyen G, Nguyen Nt, Nisar MI, Nolte S, Norheim OF, Norman RE, Norrving B, Nyakarahuka L, Odell S, O'Donnell M, Ohkubo T, Ohno SL, Olusanya BO, Omer SB, Opio JN, Orisakwe OE, Ortblad KF, Ortiz A, Otayza ML, Pain AW, Pandian JD, Panelo CI, Panniyammakal J, Papachristou C, Paternina Caicedo AJ, Patten SB, Patton GC, Paul VK, Pavlin B, Pearce N, Pellegrini CA, Pereira DM, Peresson SC, Perez-Padilla R, Perez-Ruiz FP, Perico N, Pervaiz A, Pesudovs K, Peterson CB, Petzold M, Phillips BK, Phillips DE, Phillips MR, Plass D, Piel FB, Poenaru D, Polinder S, Popova S, Poulton RG, Pourmalek F, Prabhakaran D, Qato D, Quezada AD, Quistberg DA, Rabito F, Rafay A, Rahimi K, Rahimi-Movaghar V, Rahman SU, Raju M, Rakovac I, Rana SM, Refaat A, Remuzzi G, Ribeiro AL, Ricci S, Riccio PM, Richardson L, Richardus JH, Roberts B, Roberts DA, Robinson M, Roca A, Rodriguez A, Rojas-Rueda D, Ronfani L, Room R, Roth GA, Rothenbacher D, Rothstein DH, Rowley JT, Roy N, Ruhago GM, Rushton L, Sambandam S, Søreide K, Saeedi MY, Saha S, Sahathevan R, Sahraian MA, Sahle BW, Salomon JA, Salvo D, Samonte GM, Sampson U, Sanabria JR, Sandar L, Santos IS, Satpathy M, Sawhney M, Saylan M, Scarborough P, Schöttker B, Schmidt JC, Schneider IJ, Schumacher AE, Schwebel DC, Scott JG, Sepanlou SG, Servan-Mori EE, Shackelford K, Shaheen A, Shahraz S, Shakh-Nazarova M, Shangguan S, She J, Sheikhbahaei S, Shepard DS, Shibuya K, Shinohara Y, Shishani K, Shiue I, Shivakoti R, Shrime MG,

Sigfusdottir ID, Silberberg DH, Silva AP, Simard EP, Sindi S, Singh JA, Singh L, Sioson E, Skirbekk V, Sliwa K, So S, Soljak M, Soneji S, Soshnikov SS, Sposato LA, Sreeramareddy CT, Stanaway JD, Stathopoulou VK, Steenland K, Stein C, Steiner C, Stevens A, Stöckl H, Straif K, Stroumpoulis K, Sturua L, Sunguya BF, Swaminathan S, Swaroop M, Sykes BL, Tabb KM, Takahashi K, Talongwa RT, Tan F, Tanne D, Tanner M, Tavakkoli M, Ao BT, Teixeira CM, Templin T, Tenkorang EY, Terkawi AS, Thomas BA, Thorne-Lyman AL, Thrift AG, Thurston GD, Tillmann T, Tirschwell DL, Tleyjeh IM, Tonelli M, Topouzis F, Towbin JA, Toyoshima H, Traebert J, Tran BX, Truelsen T, Trujillo U, Trillini M, Tsala Dimbuene Z, Tsilimbaris M, Tuzcu EM, Ubeda C, Uchendu US, Ukwaja KN, Undurraga EA, Vallely AJ, van de Vijver S, van Gool CH, Varakin YY, Vasankari TJ, Vasconcelos AM, Vavilala MS, Venketasubramanian N, Vijayakumar L, Villalpando S, Violante FS, Vlassov VV, Wagner GR, Waller SG, Wang J, Wang L, Wang X, Wang Y, Warouw TS, Weichenthal S, Weiderpass E, Weintraub RG, Wenzhi W, Werdecker A, Wessells KR, Westerman R, Whiteford HA, Wilkinson JD, Williams TN, Woldeyohannes SM, Wolfe CD, Wolock TM, Woolf AD, Wong JQ, Wright JL, Wulf S, Wurtz B, Xu G, Yang YC, Yano Y, Yatsuya H, Yip P, Yonemoto N, Yoon SJ, Younis M, Yu C, Yun Jin K, Zaki Mel S, Zamakhshary MF, Zeeb H, Zhang Y, Zhao Y, Zheng Y, Zhu J, Zhu S, Zonies D, Zou XN, Zunt JR, Vos T, Lopez AD, Murray CJ. GBD 2013 Mortality and Causes of Death Collaborators. Global, regional, and national age-sex specific all-cause and cause-specific mortality for 240 causes of death, 1990-2013: a systematic analysis for the Global Burden of Disease Study 2013. Lancet 2015; 385: 117-71.

[2] Minchinton AI, Tannock IF. Drug penetration in solid tumours. Nat Rev Cancer 2006; 6: 583-92.

[3] Son D, Lee J, Qiao S, Ghaffari R, Kim J, Lee JE, Song C, Kim SJ, Lee DJ, Jun SW, Yang S, Park M, Shin J, Do K, Lee M, Kang K, Hwang CS, Lu N, Hyeon T, Kim DH. Multifunctional wearable devices for diagnosis and therapy of movement disorders. Nat Nanotechnol 2014; 9: 397-404.

[4] Yu MK, Park J, Jon S. Targeting strategies for multifunctional nanoparticles in cancer imaging and therapy. Theranostics 2012; 2: 3.

[5] Chen Y, Chen H, Shi J. In Vivo Bio-Safety Evaluations and Diagnostic/Therapeutic Applications of Chemically Designed Mesoporous Silica Nanoparticles. Adv Mater 2013; 25: 3144-76.

[6] Zhang X, Zhang X, Wang S, Liu M, Zhang Y, Tao L, Wei Y. Facile incorporation of aggregation-induced emission materials into mesoporous silica nanoparticles for intracellular imaging and cancer therapy. ACS Appl Mater Interfaces 2013; 5: 1943-7.

[7] Feng W, Nie W, He C, Zhou X, Chen L, Qiu K, Wang W, Yin Z. Effect of pH-responsive alginate/chitosan multilayers coating on delivery efficiency, cellular uptake and biodistribution of mesoporous silica nanoparticles based nanocarriers. ACS Appl Mater Interfaces 2014; 6: 8447-60.

[8] Li H, Tan LL, Jia P, Li QL, Sun YL, Zhang J, et al. Near-infrared light-responsive supramolecular nanovalve based on mesoporous silica-coated gold nanorods. Chem Sci 2014; 5: 2804-8.

[9] Li Z, Barnes JC, Bosoy A, Stoddart JF, Zink JI. Mesoporous silica nanoparticles in biomedical applications. Chemical Soc Rev 2012; 41: 2590-605.

[10] Cuenca AG, Jiang H, Hochwald SN, Delano M, Cance WG, Grobmyer SR. Emerging implications of nanotechnology on cancer diagnostics and therapeutics. Cancer 2006; 107: 459-66.

[11] Farokhzad OC, Langer R. Nanomedicine: developing smarter therapeutic and diagnostic modalities. Adv Drug Deliv Rev 2006; 58: 1456-9.

[12] Egeblad M, Werb Z. New functions for the matrix metalloproteinases in cancer progression. Nat Rev Cancer 2002; 2: 161-74.

[13] Kessenbrock K, Plaks V, Werb Z. Matrix metalloproteinases: regulators of the tumor microenvironment. Cell 2010; 141: 52-67.

[14] Chen WH, Xu XD, Jia HZ, Lei Q, Luo GF, Cheng SX, Zhuo RX, Zhang XZ. Therapeutic nanomedicine based on dual-intelligent functionalized gold nanoparticles for cancer imaging and therapy in vivo. Biomaterials 2013; 34: 8798-807.

[15] Chen AM, Zhang M, Wei D, Stueber D, Taratula O, Minko T, He H. Co-delivery of Doxorubicin and Bcl-2 siRNA by Mesoporous Silica Nanoparticles Enhances the Efficacy of Chemotherapy in Multidrug-Resistant Cancer Cells. Small 2009; 5: 2673-7.

[16] Wang J, Gao PP, Yang XX, Wang TT, Wang J, Huang CZ. Real-time imaging of intracellular drug release from mesoporous silica nanoparticles based on fluorescence resonance energy transfer. J Mater Chem B 2014; 2: 4379-86.

[17] He X, Wu X, Wang K, Shi B, Hai L. Methylene blue-encapsulated phosphonate-terminated silica nanoparticles for simultaneous *in vivo* imaging and photodynamic therapy. Biomaterials 2009; 30: 5601-9.

[18] Abbad S, Wang C, Waddad AY, Lv H, Zhou J. Preparation, in vitro and in vivo evaluation of

polymeric nanoparticles based on hyaluronic acid-poly (butyl cyanoacrylate) and D-alpha-tocopheryl polyethylene glycol 1000 succinate for tumor-targeted delivery of morin hydrate. Int J Nanomedicine 2015; 10: 305.

[19] Wang C, Bao X, Ding X, Ding Y, Abbad S, Wang Y, Li M, Su Y, Wang W and Zhou J. A multifunctional self-dissociative polyethyleneimine derivative coating polymer for enhancing the gene transfection efficiency of DNA/polyethyleneimine polyplexes in vitro and in vivo. Polymer Chemistry 2015; 6: 780-796.

[20] Tian T, Nan KJ, Guo H, Wang WJ, Ruan ZP, Wang SH, Liang X, Lu CX. PTEN inhibits the migration and invasion of HepG2 cells by coordinately decreasing MMP expression via the PI3K/Akt pathway. Oncol Rep 2010; 23: 1593-600.

[21] Kalaria D, Sharma G, Beniwal V, Kumar MR. Design of biodegradable nanoparticles for oral delivery of doxorubicin: in vivo pharmacokinetics and toxicity studies in rats. Pharm Res 2009; 26: 492-501.